

Original Article

Contribution of Lewis X Carbohydrate Structure to Neuropathogenic Murine Coronaviral Spread

Masatoshi Kakizaki¹, Akira Togayachi², Hisashi Narimatsu², and Rihito Watanabe^{1*}

¹*Department of Bioinformatics, Graduate School of Engineering, Soka University, Tokyo 192-8577; and*

²*Glycoscience and Glycotechnology Research Group, Biotechnology Research Institute for Drug Discovery, National Institute of Advanced Industrial Science and Technology (AIST), Ibaraki 305-8568, Japan*

SUMMARY: Although Lewis X (Le^x), a carbohydrate structure, is involved in innate immunity through cell-to-cell and pathogen recognition, its expression has not been observed in mouse monocytes/macrophages (Mo/Mas). The Mo/Mas that infiltrate the meninges after infection with the neuropathogenic murine coronavirus strain *srr7* are an initial target of infection. Furthermore, higher inflammatory responses were observed in gene-manipulated mice lacking α 1,3-fucosyltransferase 9, which determines the expression of the Le^x structure, than in wild type mice after infection. We investigated Le^x expression using CD11b-positive peritoneal exudate cells (PECs) and found that Le^x is inducible in Mo/Mas after infection with *srr7*, especially in the syncytial cells during the late phase of infection. The number of syncytial cells was reduced after treatment of the infected PECs with anti-Le^x antibody, during the late phase of infection. In addition, the antibody treatment induced a marked reduction in the number of the infected cells at 24 hours post inoculation, without changing the infected cell numbers during the initial phase of infection. These data indicate that the Le^x structure could play a role in syncytial formation and cell-to-cell infection during the late phase of infection.

INTRODUCTION

cl-2 virus (cl-2), isolated from a neuropathogenic murine coronavirus mouse hepatitis virus (MHV) strain, JHM virus (JHM) (1), exhibits extremely high neurovirulence after infection, leading infected mice to morbid states within 3 days post-inoculation (dpi), without inducing demyelination in the white matter of the brain that is observed with other JHMs (2). Instead, it produces necrotic lesions in the grey matter with infected neurons, which do not express the major MHV receptor carcinoembryonic antigen-related cell adhesion molecule 1 (CEACAM1) (3,4). A mutant clone isolated from cl-2, *srr7*, shows attenuated neurovirulence compared to cl-2, although its virulence is still higher than that of the other JHMs, exhibiting rapid viral spread from one organ to another non-adjacent organ within 12 hours after infection, designated as super-acute spread (5). Most of the mice infected with *srr7* survive for more than 7 days and die within 10 dpi. The viral antigens in the brain are detectable in the white matter. However, the neuropathological characteristics are not demyelinating inflammation, but spongiosis, which appears 48 hours post-inoculation (hpi) (6). Initial viral antigens, after inoculation with either cl-2 or *srr7*, are detectable in CD11b- or F4/80-positive monocytes/macrophages (Mo/Mas) that have infiltrated the meninges. Syncytial giant cells formed of infected Mo/

Mas are often found in the meninges and ventricular cavity (5).

The neuropathological lesions in the brain, including demyelination (7,8), induced by JHM infection are considered to be, to some extent, the results of an indirect mechanism of infection. *srr7* induces spongiotic lesions in areas where no viral antigens are detectable during the early phase of infection (6), without prominent inflammation, but with elevated levels of proinflammatory cytokines in the infected brain (9). Damage of neurons in the hippocampus was reported to result from bystander effects of infection with Mu-3, a mutant isolated from *srr7* (10), and another kind of virus, such as Theiler's murine encephalomyelitis virus (TMEV) (11). Mechanisms of human brain injuries after infection with human immunodeficiency virus (12), human T-cell leukemia virus I (13), measles virus (14), and influenza virus (15) have also been discussed from the perspective of immune-triggered bystander effects.

In the bystander lesions, an antigenic epitope with a Lewis X (Le^x: galactose β 1-4 Fucose α 1-3) N-acetylglucosamine carbohydrate structure was recently found to be involved in infection with *srr7*, in mutant mice that lack the gene encoding α 1,3-fucosyltransferase 9 (FUT9) (9). FUT9 determines the final structure of Le^x and the gene-manipulated mice *Fut9*^{-/-} reportedly do not express Le^x (16). However, we failed to clearly detect *in vivo* Le^x expression in the infected organs, including the spleen and brain, of wild type mice. The result might be a false negative due to procedures to prepare sections from tissues for immunohistochemistry. Therefore, we examined Le^x expression after the infection using cultured Mo/Mas derived from peritoneal exudate cells (PECs). In this study, we showed for the first time that the Le^x structure was inducible in Mo/Mas after infection.

Received October 15, 2015. Accepted December 28, 2015.
J-STAGE Advance Publication February 19, 2016.

DOI: 10.7883/yoken.JJID.2015.499

*Corresponding Author: Mailing address: Department of Bioinformatics, Graduate School of Engineering, Soka University, Tangi-cho, Hachioji, Tokyo 192-8577, Japan. Tel and Fax: +81-426-9465, E-mail: rihitow@soka.ac.jp

MATERIALS AND METHODS

Viruses and Animals: A neuropathogenic MHV strain, srr7, was used in this study. This virus was propagated and titrated in DBT cells maintained in Dulbecco's modified Eagle's minimal essential medium (Gibco, Grand Island, NY, USA) supplemented with 5% heat-inactivated fetal bovine serum (FBS; Sigma, Tokyo, Japan), as previously described (17). Specific pathogen-free inbred BALB/c mice purchased from Charles River (Tokyo, Japan) were housed in a specific pathogen-free animal facility and maintained according to the guidelines set by the ethical committee of our university. For the experiment, mice were transferred to a biosafety level 3 (BSL-3) laboratory, after permission from the committee of our university. Six to seven-week-old mice were used for all experiments.

Preparation of peritoneal exudate cells: Thioglycollate medium (TM) was prepared by dissolving 20 g of Brewer thioglycollate (TG) medium (BD Diagnostics, Loveton Circle Sparks, MD, USA), supplemented with 10.0 g of proteose peptone (BD Diagnostics), 2.38 g of sodium chloride (Wako, Osaka, Japan), and 0.945 g of dipotassium phosphate (Wako), in 1,000 ml of distilled water to obtain a TM with components similar to those of the classical product provided by Difco Laboratories (Detroit, MI, USA) (18). TM was autoclaved for 20 min at 15 lbs of pressure at 121°C, and was kept in the dark under sterile conditions at room temperature. Four days after the injection of 2 mL of TM into the peritoneal cavity, the peritoneal cavity was washed with phosphate-buffered saline (PBS; Nissui, Tokyo, Japan), and PECs were collected. To obtain adherent PECs, the

cells were seeded at 2×10^5 cells per well in 8-well glass-bottom chamber slides (Nalge Nunc International, Rochester, NY, USA), and were cultured in the RPMI 1640 medium (Gibco) supplemented with 10% heat-inactivated FBS (Gibco). After 24 hours, the adherent cells were inoculated with 1.3×10^3 or 6.5×10^3 plaque-forming units (PFU) of srr7 virus per well and incubated for a specified time. To prepare PECs for flow cytometric analysis, they were cultured in suspension for 24 hours at 2×10^7 cells in 1 mL of the medium described above, in 1.5-mL microtubes, with continuous rotation at 20 rpm.

Assay of adherent PECs: For immunostaining, adherent PECs were fixed in cold ethanol on chamber slides for 1 min, followed by fixation in cold acetone for 5 min; antibodies and reagents listed in Table 1 were used. Cell cultures labeled with fluorescent dyes were mounted with a gold antifade reagent (Invitrogen, Carlsbad, CA, USA). Fluorescence was visualized under either a confocal laser scanning microscope (Leica Microsystems, Heidelberg, Germany) or a fluorescence microscope (Keyence, Osaka, Japan). The number of infected cells was counted using the BZ analyzer (Keyence). For the inhibition test, either mouse anti-Lewis X mAb (1 : 100) or mouse anti-Sialyl-Lewis X mAb (1 : 100) (Table 1) was added to the culture medium.

Flow cytometry: After incubating suspension culture for 24 hours, PECs were inoculated with 1.3×10^5 PFU of srr7 virus and were cultured for further 24 hours. Subsequently, the PECs were washed twice in PBS and resuspended in fluorescence-activated cell sorting (FACS) buffer, which contains 1% bovine serum

Table 1. Antibodies and reagents used in this study

Target	Species	Clone or designation	Conjugate	Reference/supplier
Primary antibodies for immunofluorescence staining				
JHMV	Rabbit	Polyclonal	Purified	3
Gr-1	Rat	RB6-8C5	Biotin	BioLegend, San Diego, CA, USA
CD11b	Rat	M1/70	Biotin	BD Pharmingen, San Diego, CA, USA
F4/80	Rat	BM8	Purified	eBioscience, San Diego, CA, USA
Le ^x	Mouse	MC480	Purified	Developmental Studies Hybridoma Bank, University of Iowa, Ames, IA, USA
FUT9	Mouse	Monoclonal	Purified	22
Sialyl-Le ^x	Mouse	CSLEX1	Purified	BD Biosciences, San Jose, CA, USA
Primary antibodies for flow cytometry				
Gr-1	Rat	RB6-8C5	FITC	eBioscience
CD11b	Rat	M1/70	PE	eBioscience
F4/80	Rat	BM8	APC	eBioscience
Secondary antibodies for immunofluorescence staining				
Rabbit IgG	Sheep	Polyclonal	FITC	Abcam, Tokyo, Japan
Rat IgG	Donkey	Polyclonal	Alexa568	Abcam
Mouse IgG	Goat	Polyclonal	Alexa488	Molecular Probe, Carlsbad, CA, USA
Mouse IgG	Donkey	Polyclonal	Biotin	Rockland, Gilbertsville, PA, USA
Streptavidin			Alexa488	Invitrogen, Carlsbad, CA, USA
Streptavidin			Alexa568	Invitrogen
Reagent to stain nuclei				
Hoechst33342				Invitrogen
Antibodies for inhibition assay of Le ^x				
Le ^x	Mouse	MC480	Purified	Developmental Studies Hybridoma Bank
Sialyl-Le ^x	Mouse	CSLEX1	Purified	BD Biosciences

Gr-1, granulocyte-differentiation antigen-1; FITC, Fluorescein isothiocyanate; PE, Phycoerythrin; APC, Allophycocyanin.

albumin (BSA; Sigma) and 0.1% NaN₃ in PBS. For phenotypic analysis, 1×10^6 cells for each staining were initially incubated with Fc block (BD Biosciences, San Jose, CA, USA) ($5 \mu\text{g}/\text{mL}$) for 20 min at 4°C. Subsequently, the cells were incubated with the appropriate fluorochrome-conjugated antibodies (Table 1) for 30 min at 4°C, followed by 3 washes with FACS buffer, and were acquired on a FACS Calibur (BD Biosciences). Appropriate isotype controls were used in all cases. Data were analyzed using FlowJo software (Tree Star, Jackson, OR, USA).

RESULTS

Population and susceptibility of PECs: The PECs that we used were collected after the injection of TM into the peritoneal cavity, and were expected to be mixed populations of leukocytes (19,20). FACS analysis revealed high expressions of CD11b and F4/80 in 50–70% of the PECs (Fig. 1). Around 35% of the PECs were Gr-1-positive (Fig. 1). After viral inoculation, the population appeared grossly similar. However, on double staining for CD11b and Gr-1 (CD11b:Gr-1), a small population (Fig. 1B) showed a relatively high expression of both antigens after infection. Based on F4/80:Gr-1 (Fig. 1B) and F4/80:CD11b (Fig. 1A), similar shifts of the population were observed with the upregulation of Gr-1 and CD11b, respectively, without a significant change in the F4/80 expression level after infection. The PECs attached to the culture glass slides, examined by immunofluorescence staining (IF), also exhibited high expression rates of CD11b and F4/80, in around 70% and 40% of PECs, respectively (Fig. 2A). The population of Gr-1-positive cells among PECs was around 20%. After the inoculation, the population of PECs did not show a marked difference compared to that of culture without viral inoculation (Fig. 2A). Through the inoculation of 2×10^5 PECs with 1.3×10^3 PFU of sr7, the PECs were found to be susceptible to sr7 infection. The infected area in the culture plate spread rapidly between 12 and 24 hpi (Fig. 2B) forming syncytia (Fig. 3), all of which bore viral antigens (Fig. 4). A few syncytia had already formed before 12 hpi (Fig. 5C). The susceptibility of PECs to sr7 seemed to be comparable to that of DBT cells, which have been used to prepare virus stock with a high titer (5), because a viral inoculation with 1.3×10^3 PFU, produced and titrated using DBT cells, generated similar numbers of syncytia as in the PECs at 24 hpi (Fig. 5C). However, the level of viral production measured in the culture medium was lower in PECs compared to DBT cells, i.e., PFU at 24 hpi in PEC culture were $1\text{--}2 \times 10^2$, whereas those in DBT cell culture ranged from $5 \times 10^4\text{--}2 \times 10^5$ (data not shown).

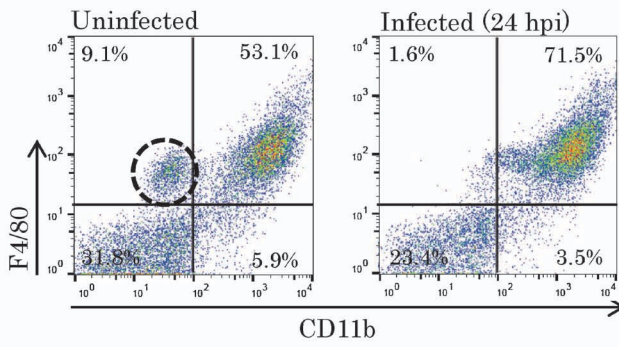
Expression of antigens in the PECs: Interestingly, most of the syncytia (>95%) showed the expression of Gr-1, which were also CD11b-positive (Fig. 3A and B). Solitary CD11b-positive (CD11b⁺) cells, which did not form syncytia with or without viral antigens, were also observed (Fig. 3A). Some CD11b⁺ and viral antigen-negative (V⁻) cells were detected extending their long foot processes and connecting to the V⁺ cells (Fig. 3A1–3). Such a connection, using the long foot process of V⁻ CD11b⁺ cells, was not detectable in Gr-1⁺ cells,

partially because most of the Gr-1⁺ cells carried viral antigens after the inoculation (Fig. 3B).

After the inoculation, Le^x antigen appeared in the PECs cultured on the glass slides (Fig. 3C), but was not detected in the mock-infected PECs (Fig. 3D). Most of the Le^x antigens were detected in the syncytial cells (Fig. 3C). Some cells with a single nucleus, bearing the Le^x antigens without viral antigen expression, were found around the syncytia (Fig. 3C). Unlike CD11b expression in the foot process of PECs, the fine projection was not traceable using anti-Le^x antibody (Fig. 4A). However, this does not mean that Le^x was not expressed there, because the available antibodies that we used failed to detect Le^x expression in monocytes, which bear CEACAM1 that has been proven to be modified by the Le^x structure (21), in the normal state (Fig. 3D). Beside CD11b⁺Le^x⁺ cells, Gr-1⁺Le^x⁺ PECs also appeared as solitary cells with a single nucleus as well as in syncytia with multiple nuclei (Fig. 4B).

FUT9, an enzyme which determines Le^x expression (22), showed a similar manner of expression in PECs after infection as Le^x, i.e. most of the FUT9-positive cells formed syncytia with multiple nuclei (Fig. 4D), which carried CD11b and Gr-1 antigens (Figs. 4C and D). FUT9 antigens were also detected in some solitary cells as well as Le^x. A noticeable difference between the Le^x and FUT9 appearance was observed after kinetic studies. At 12 hpi, Le^x was not detectable even in the syncytia (Figs. 4E1 and 2). In contrast, FUT9 antigen was detected at 12 hpi (Figs. 4E3–5). In order to examine whether or not Le^x is involved in syncytium formation, we added anti-Le^x antibody (anti-Le^x) to the PEC culture. For the control experiment, we used monoclonal antibody against sialyl-Le^x (anti-sialyl-Le^x), which detects human sialyl-Le^x, but not that of mice (23), as shown in Fig. 5A. The number of syncytia was decreased when the cultures were treated with anti-Le^x during 0–24 hpi, compared to those with anti-sialyl-Le^x treatment (Figs. 5A and C). However, the treatment with antibodies did not cause reductions in the cell numbers of the adherent cells (Figs. 5B and E). Furthermore, application of the antibody before infection did not lead to significant differences between treatments with anti-Le^x and anti-sialyl-Le^x (Figs. 5A and C). The change in the syncytial numbers after treatment with the antibody does not mean a change in the number of infected foci, in other words initial infectivity of the viruses; instead, it means a change in the number of the syncytia that grew large enough to be detectable under a light microscope. Therefore, infected foci during the early phase of infection were counted for viral antigens at 12 hpi using IF, which proved that there were no differences in the numbers of infected cells (Fig. 5D) and the numbers of syncytia (Fig. 5C) at 12 hpi, among cultures with or without these antibodies; corresponding to our previous observation (9) that viral infectivity of PECs derived from Fut9^{-/-} and wild type mice was the same. The treatment with anti-Le^x reduced the number of viral antigen-positive cells as well, when counted at 24 hpi (Fig. 5D), which indicated that the antibody inhibits not only syncytium formation but also cell-to-cell infection.

A) F4/80- and CD11b-positive population



B) Forward/side scatter profile

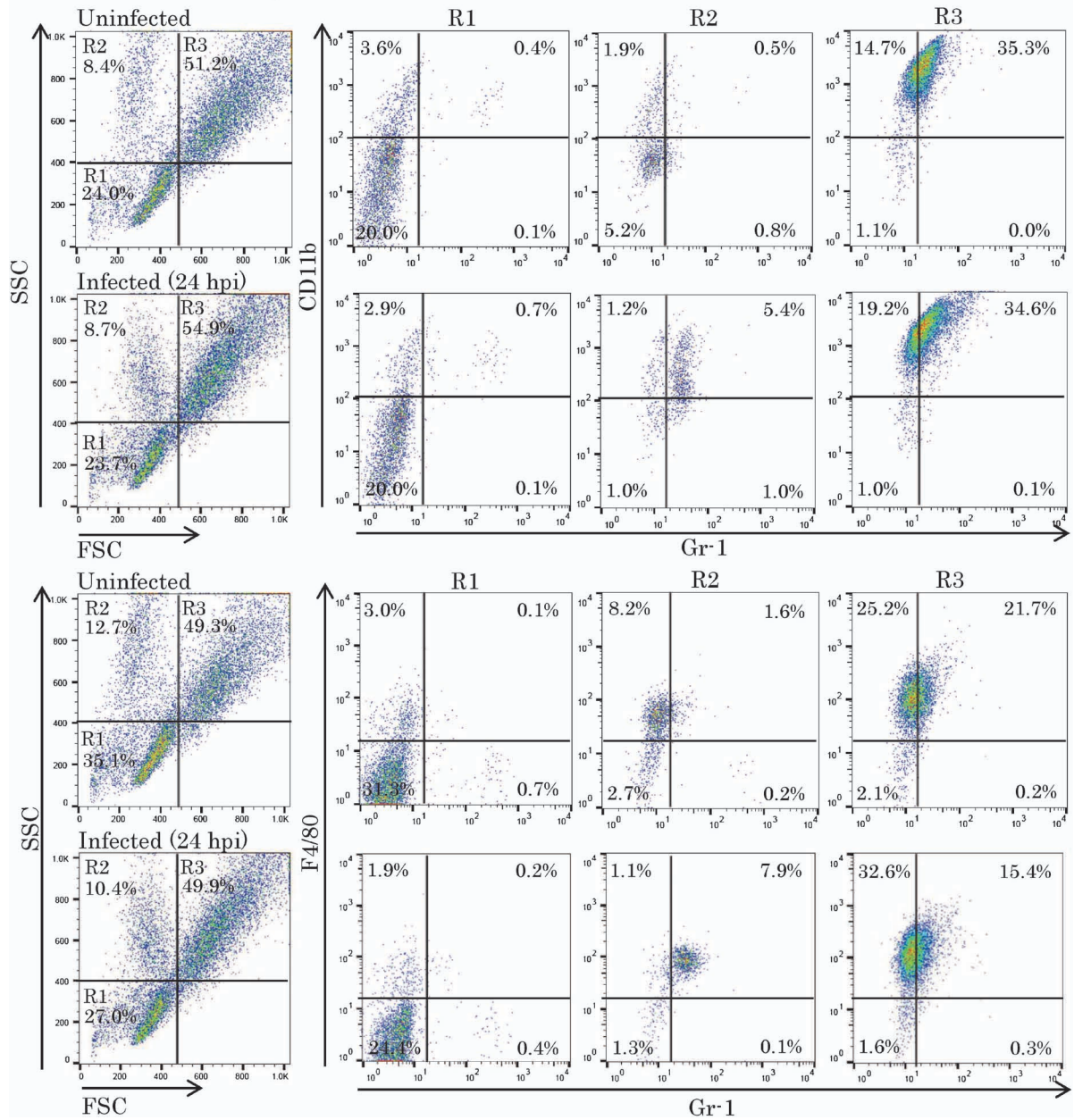


Fig. 1. (Color online) Flow cytometry of PECs in suspension culture populations of CD11b-, Gr-1-, and F4/80-positive PECs after suspension culture for 24 hours (h) with or without viral infection (Infected [24 hpi] or Uninfected, respectively) were studied by flow cytometric analysis. A): The cells in dotted circle showed a higher expression level of CD11b after infection. B): The cell populations were divided into 4 regions by forward- and side-scattering (FSC and SSC, respectively) profile. The antigen expression patterns of each region (R1-R3) are shown.

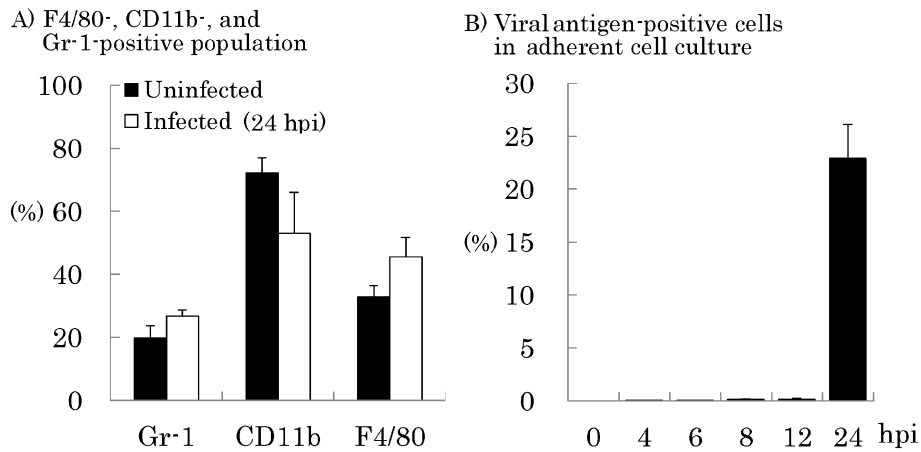


Fig. 2. Cell populations of PECs in adherent cell culture. A): Populations of CD11b-, Gr-1-, and F4/80-positive adherent PECs cultured for 24 h on chamber slides by immunofluorescent staining, with or without viral infection (24 hpi or Uninfected, respectively). B): The ratio of infected adherent PECs, detected by immunofluorescent staining for viral antigens, at desired intervals is shown. The adherent PECs were infected with 1.3×10^3 PFU of srr7 per well. Each infection was conducted in triplicate, and antigen-positive cells of each well were counted. Vertical lines indicated in the bar are the mean \pm SD.

DISCUSSION

Although TG-elicited PECs (TG-PECs) were introduced as phagocytes with high purity (24), recent studies using flow cytometry revealed that these TG-PECs have heterogeneous population of leukocytes (19). Even macrophages, identified as CD11b^{hi}F4/80^{hi-int}, after gating out B cells, neutrophils, eosinophils, and DCs from the TG-PECs through flow cytometry, appeared heterogeneous, based on the expression of MHC II and Ly6C antigens (20). Various populations of macrophages among TG-PECs have been reported depending upon the gating strategy, including side- or forward-scatter profiles using flow cytometry, or the efficiency of the antibodies used (25). The report of 86–95% macrophages in the TG-PECs (26–28) was criticized as an overestimation by the research group of Misharin (20), who claimed that only 40–45% macrophages and as high as 30–40% eosinophils comprise TG-PECs. Similarly, reports on the population of Gr-1-positive cells in the TG-PECs range from 1% (19) to 40% (20). Our estimated populations of CD11b⁺, F4/80⁺, or Gr-1⁺ cells in the TG-PECs fell into the ranges reported previously. Gr-1⁺ cells among the TG-PECs were 20–35%.

These PECs, composed of heterogeneous cell populations, were found to be susceptible to Srr7 infection with a similar efficiency compared to DBT cells, which are used for the titration of MHV. It should be noted that most of the syncytia formed after infection of TG-PECs expressed Gr-1 antigen. The main target among leukocytes of MHV-JHM infection has been believed to be the lineages of Mo/Mas, including microglia in the brain (5,29), which express CEACAM1. CEACAM1 is also detectable as an adhesion molecule on Gr-1-positive human granulocytes (22). However, it has not been reported that Gr-1-positive cells are the main targets of MHV infection. To determine whether the colocalization of viral and Gr-1 antigens occurred through preferential viral infectivity of Gr-1⁺ cells, further studies need to be conducted, because Gr-1 antigen might be inducible by endogenous or exogenous factors (30).

Actually, we observed that a small population, with polymorphism among PECs, (Fig. 1B) showed higher Gr-1 expression after infection compared to that detected before infection.

Among these Gr-1-positive cells, Le^x and FUT9 antigen expressions were induced after infection. The antigens were detected predominantly in the infected Gr-1- and CD11b-positive cells, which formed syncytia. The synthesis of Le^x was not involved in the initial formation of syncytia, because Le^x-positive syncytia appeared during the late phase of infection and the inhibition of syncytium formation by anti-Le^x was detected during the late phase of infection, but not during the early phase. The Le^x carbohydrate structure does not affect the initial viral infectivity of TG-PECs, because the pre-incubation of TG-PECs with anti-Le^x did not change the number of the infected cells, and the TG-PECs derived from Fut9^{-/-} mice, which do not express Le^x (16), showed the same infectivity as those from wild type mice (9). Therefore, it is indicated that the Le^x structure decorating CEACAM1 has no contribution to the attachment of the virus. A possibility that this structure was involved in the increase in Le^x antigen expression is unlikely, because we did not observe any increase in the CEACAM1 expression after infection, using IF (data not shown). Rather, the expression of the receptor could have been downregulated, like in other kinds of viral infections, including one with human coronavirus (31).

In addition to the roles during development, the Le^x carbohydrate structure, known as stage-specific embryonic antigen-1 (16), is involved in innate immunity through cell-to-cell and pathogen recognition (21,32–34). Dynamic immune regulation is induced after interaction between Le^x carbohydrate structures and lectins serving as C-type lectin receptors (35), which include scavenger receptor with C-type lectin (SRCL), human dendritic cell-specific intercellular adhesion molecule-3-grabbing non-integrin (DC-SIGN), and its mouse homologue SIGN-related-1 (SIGNR1) (36,37). This CRL-mediated signaling can be turned to a pro- (37) or anti-inflammatory status (38,39) depending on

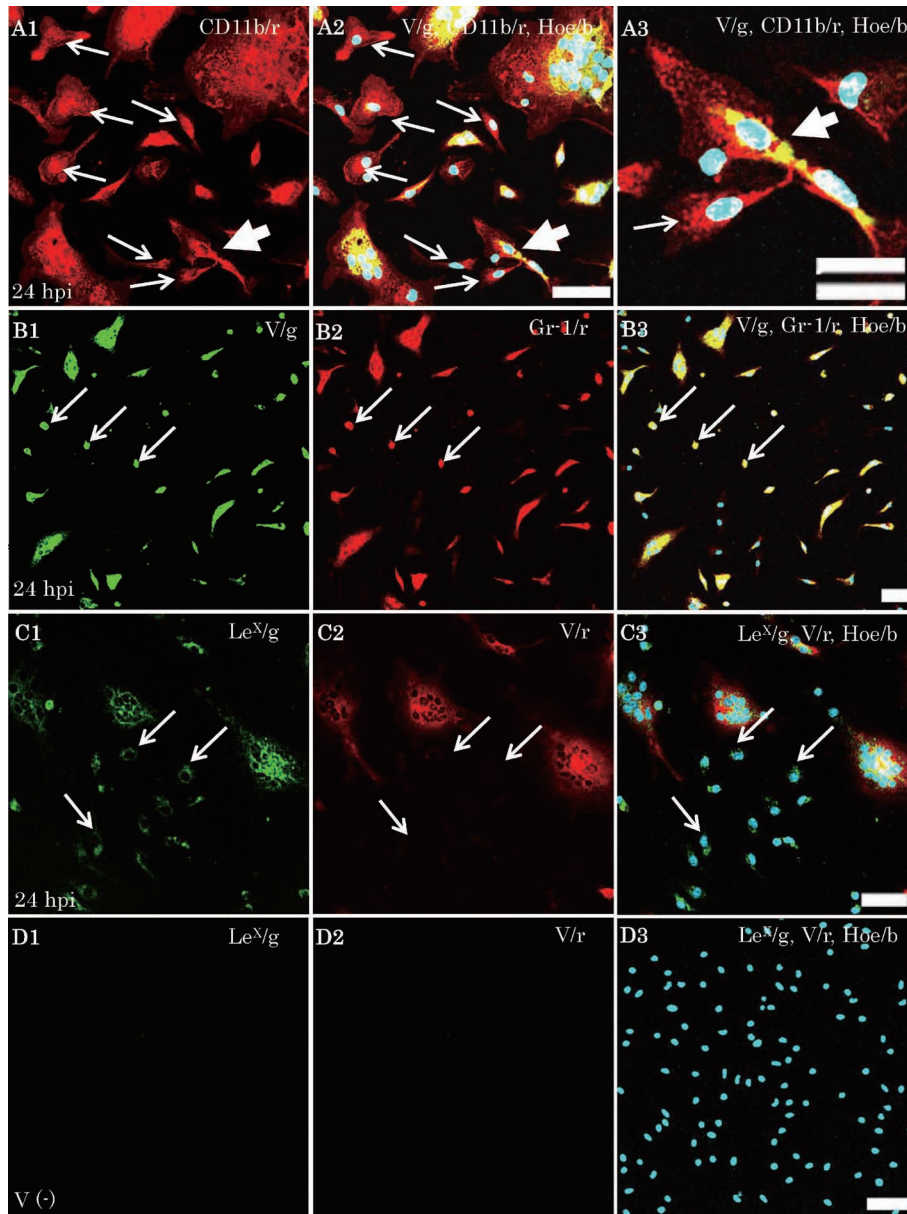


Fig. 3. (Color online) Antigen expression in the syncytia and solitary cells. Twenty-four hours after seeding PECs on 8-well chamber slides, the cultured cells were infected with 1.3×10^3 PFU of *srr7* per well, or left uninfected (V[-]). At 24 hpi, culture slides were processed to detect JHMV (V, A-D), CD11b (A), Gr-1(B), and Lewis X (Le^x , C and D) antigens. Hoechst 33342 (Hoe) was used for nuclear counter-staining, which is shown as a digital blue color (/b). Digital red and green colors are indicated as /r and /g in the pictures, respectively. Note that around syncytia are solitary Gr-1 or CD11b-positive cells not forming syncytia (A and B). Around syncytia, most of the solitary CD11b-positive cells were not infected (narrow arrows in A), whereas all solitary Gr-1-positive cells were infected (narrow arrows in B). Some of these solitary cells around the syncytia projected long foot processes connected with syncytia (bold arrows in A, shown at a higher magnification in A3). At 24 hpi, Le^x antigens were detected in the syncytial cells (C). A few uninfected cells with a single nucleus around syncytia expressed Le^x (narrow arrows in C). In the mock-infected PECs, Le^x antigens were not detected (D). White single and double bars indicate 50 and 25 μ m, respectively.

the glycan composition or agents that trigger the immune reaction. Our previous study indicated that Le^x expression is involved in signaling that negatively influences the immune responses in the course of *srr7* infection using *Fut9^{-/-}* mice. In addition, the *Fut9^{-/-}* mice, which do not express Le^x , showed extended inflammatory responses compared to wild type mice (9), which exhibited a poor inflammatory reaction in the infected brain accompanied by a reduced population of leukocytes in the spleen, after infection with *srr7* (40).

In spite of these important roles of Le^x carbohydrate structures in immune response, the expression of Le^x has not been detected by IF or flow cytometry in mouse leukocytes, even in monocytes, which express CEACAM1. However, it has been demonstrated, by mass spectrometry, that CEACAM1 carries rich Le^x carbohydrate structures (21). One of the reasons may be that the most sensitive anti- Le^x antibody we examined was of the IgM class, which might be too large to access antigenic sites that are covered by a tertiary conformation of pro-

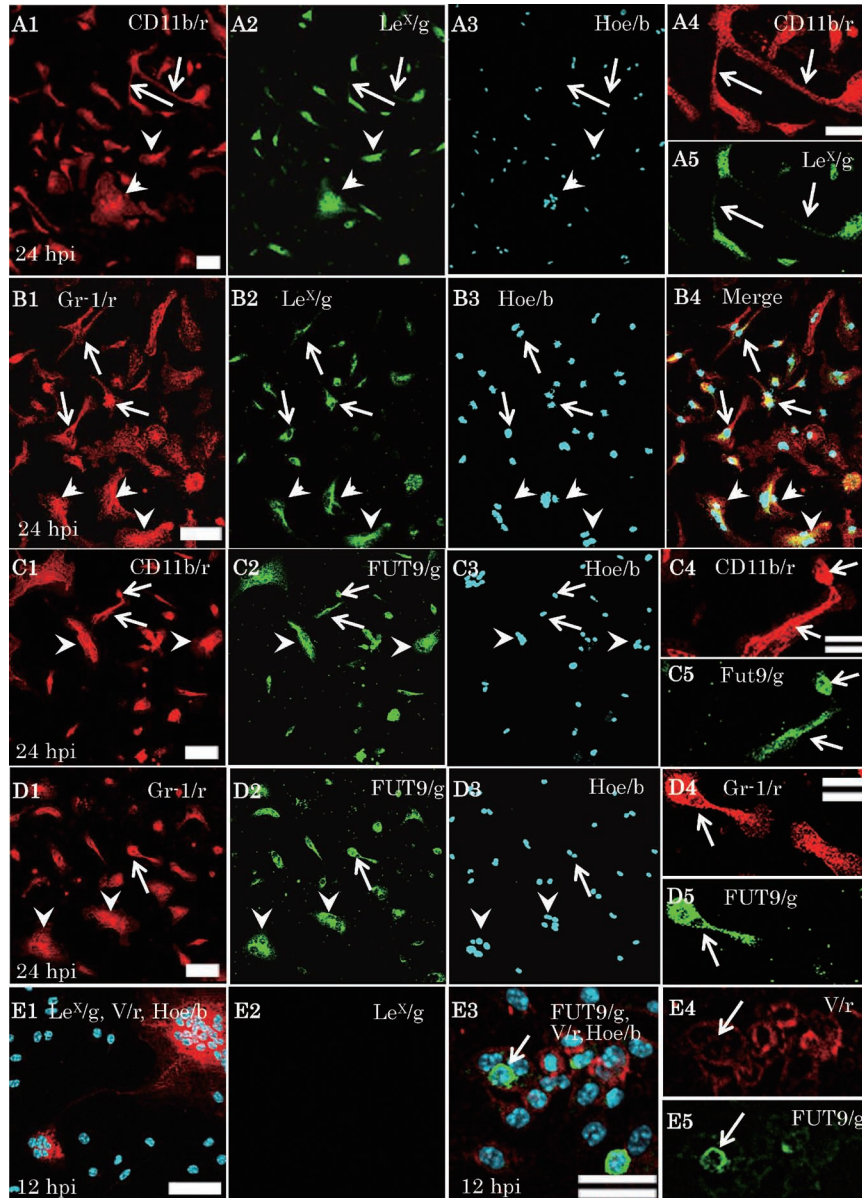


Fig. 4. (Color online) Expressions of Le^x and Fut9. Adherent PECs on culture slides were stained with Lewis X (Le^x ; A, B, E1, and E2), CD11b (A and C), Gr-1 (B and D), JHMV (V; E), and Fut9 (D and E3-E5) antigens at 12 hpi (E) and 24 hpi (A-D). Hoechst 33342 (Hoe) was used for nuclear counter-staining, which is shown as a digital blue color (/b). Digital red and green colors are indicated as /r and /g in the pictures, respectively. At 24 hpi, most of the CD11b- or Gr-1-positive syncytia carried Le^x (arrowheads in A and B) or FUT9 (arrowheads in C and D) antigens. Le^x or FUT9 antigens were also detected in some solitary cells (narrow arrows in B-D). The CD11b-positive fine projection (narrow arrows in A1) was not traceable using anti- Le^x antibody (A2), shown at a higher magnification (A4 and A5). At 12 hpi, Le^x was not detected even in syncytia (E1 and E2), whereas Fut9 was detected in the initial small syncytia at 12 hpi (narrow arrows in E3-5). White single and double bars indicate 50 and 25 μm , respectively.

teins or other carbohydrates. Nevertheless, we showed that highly expressed Le^x was detected in the syncytia and satellite cells (SCs) around the syncytia using Mo/Mas attached to glass slides, which could have been beneficial for the antibodies to reach the antigenic sites in the Mo/Mas, with a fairly well-preserved cell architecture after fixation procedures were employed on the cells attached to the glass slides (41). Furthermore, using Mo/Mas attached to glass slides, we could detect that some SCs projected long foot processes connecting to syncytia, mimicking immune synapse, enabling cross-talk between leukocytes several hundred μm apart (42).

The connection, through foot processes, between SCs and initial small syncytia might be necessary for them to grow large enough to become detectable with a light microscope, during the late phase of infection, and Le^x might be involved in this process. Expression levels detectable by IF during extremely virulent viral infections would provide an opportunity to clarify the functional roles of Le^x and its lectins, during infection and immune responses directed not only by mature Mo/Mas but also by dendritic cells, because TG-PECs contain immature $CD11b^+Gr-1^+$ cells that can differentiate into dendritic cells (43). Furthermore, among these $CD11b^+Gr-1^+$

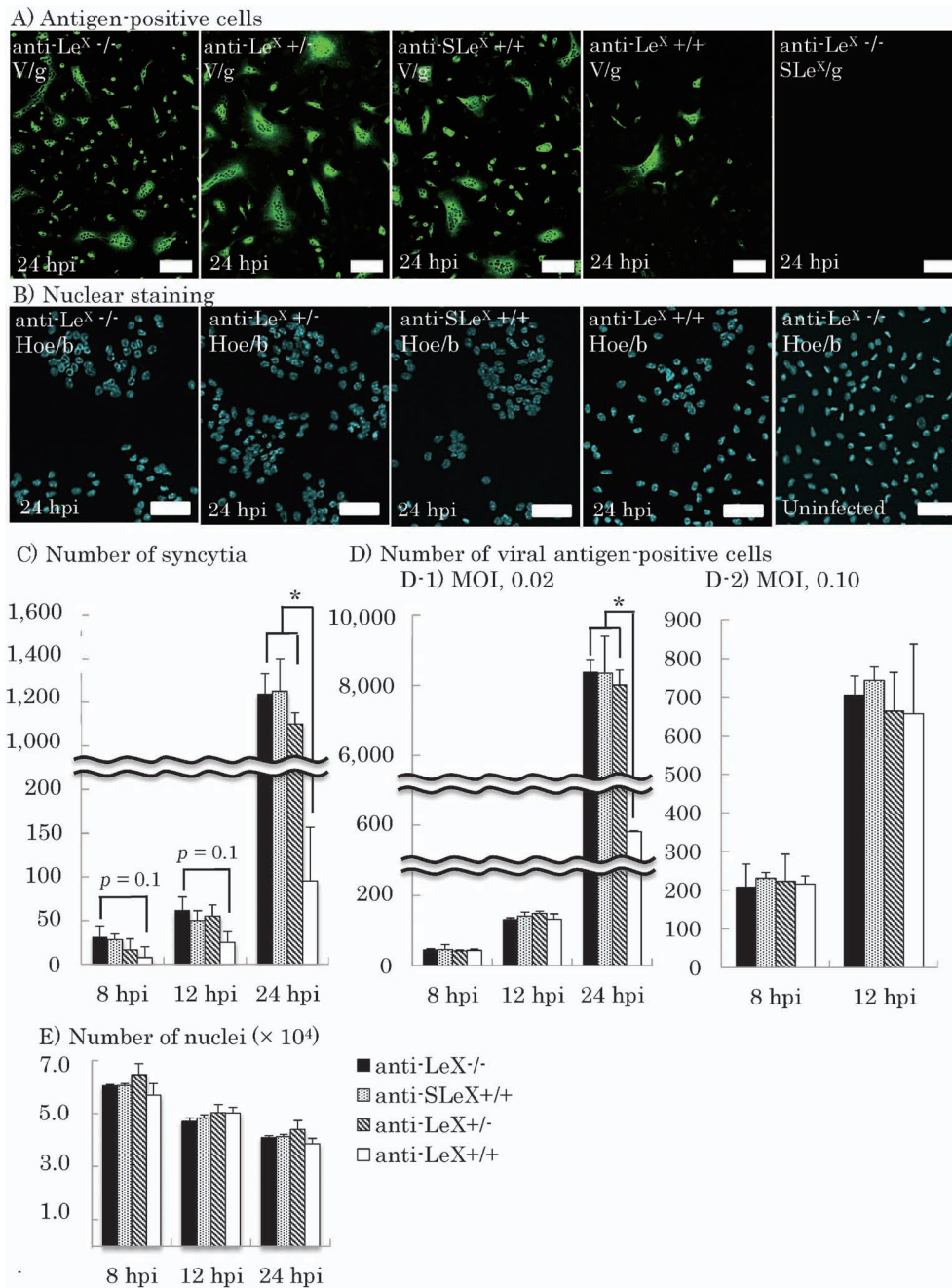


Fig. 5. (Color online) Effects of anti- Le^x antibody. Anti- Le^x (anti- Le^x) or anti-S Le^x (anti-S Le^x) antibody were added to the PEC culture well before viral inoculation for 1 hour (+/) and at the time of inoculation (/+), or PECs were cultured without treatment with the antibodies (designated as -/ or /-, depending on the periods of culture, that is before or after viral inoculation, respectively). Virus was inoculated at an M.O.I of 0.02 (MOI, 0.02) through the experiments except for D-2) to count viral antigen positive cells during the early phase of infection at a higher M.O.I. (MOI, 0.1) (A) and B): Immunofluorescent staining for viral antigens (V/g) and S Le^x (S Le^x /g) (A), or nuclear staining using Hoechst33324 (Hoe) (B)), with viral infection at 24 hpi (24 hpi) or without (Uninfected). White single bar indicates 50 μ m. C), D), and E): Culture slides were processed for immunofluorescent staining for viral antigens (C) and D)) or nuclear staining (E), and photographed using a fluorescent microscope (Keyence). The number of viral antigen-positive cells or nuclei was counted using a BZ analyzer (Keyence). A syncytium was identified when a viral antigen-positive cell had more than 3 nuclei with a major cytoplasmic axis of more than 50 μ m. Each experiment was conducted in triplicate, and viral antigen-positive cells or nuclear numbers in each well were counted. p , P -value by Student's t -test. Asterisks indicate $p < 0.05$. Vertical lines are the mean \pm SD.

precursor cells, there are myeloid-derived suppressor cells (MDSC) (30), which might expand their population, after extremely virulent viral infection, to contribute to a rapid spread of the viruses. A small population detected by flow cytometry as a shifted population after infection, with elevated expression of CD11b⁺ and

Gr-1⁺, may be a candidate for MDSC. The detection of Le^x expression in the population is in progress in our laboratory.

Acknowledgments We thank Ms Nami Suzuki of National Institute

of Advanced Industrial Science and Technology for technical support to flow cytometric analysis.

Conflict of interest None to declare.

REFERENCES

1. Taguchi F, Siddell SG, Wege H, et al. Characterization of a variant virus selected in rat brains after infection by coronavirus mouse hepatitis virus JHM. *J Virol.* 1985;54:429-35.
2. Bender SJ, Weiss SR. Pathogenesis of murine coronavirus in the central nervous system. *J Neuroimmune Pharmacol.* 2010;5:336-54.
3. Matsuyama S, Watanabe R, Taguchi F. Neurovirulence in mice of soluble receptor-resistant (srr) mutants of mouse hepatitis virus: intensive apoptosis caused by less virulent srr mutant. *Arch Virol.* 2001;146:1643-54.
4. Godfraind C, Langreth SG, Cardellicchio CB, et al. Tissue and cellular distribution of an adhesion molecule in the carcinoembryonic antigen family that serves as a receptor for mouse hepatitis virus. *Lab Invest.* 1995;73:615-27.
5. Takatsuki H, Taguchi F, Nomura R, et al. Cytopathy of an infiltrating monocyte lineage during the early phase of infection with murine coronavirus in the brain. *Neuropathology.* 2010;30:361-71.
6. Kashiwazaki H, Nomura R, Matsuyama S, et al. Spongiform degeneration induced by neuropathogenic murine coronavirus infection. *Pathol Int.* 2011;61:184-91.
7. Glass WG, Chen BP, Liu MT, et al. Mouse hepatitis virus infection of the central nervous system: chemokine-mediated regulation of host defense and disease. *Viral Immunol.* 2002;15:261-72.
8. Glass WG, Hickey MJ, Hardison JL, et al. Antibody targeting of the CC chemokine ligand 5 results in diminished leukocyte infiltration into the central nervous system and reduced neurologic disease in a viral model of multiple sclerosis. *J Immunol.* 2004;172:4018-25.
9. Kashiwazaki H, Kakizaki M, Ikehara Y, et al. Mice lacking $\alpha 1,3$ -fucosyltransferase 9 exhibit modulation of in vivo immune responses against pathogens. *Pathol Int.* 2014;64:199-208.
10. Kakizaki M, Kashiwazaki H, Watanabe R. Mutant murine hepatitis virus-induced apoptosis in the hippocampus. *Jpn J Infect Dis.* 2014;67:9-16.
11. Buenz EJ, Sauer BM, Lafrance-Corey RG, et al. Apoptosis of hippocampal pyramidal neurons is virus independent in a mouse model of acute neurovirulent picornavirus infection. *Am J Pathol.* 2009;175:668-84.
12. Mattson MP, Haughey NJ, Nath A. Cell death in HIV dementia. *Cell Death Differ.* 2005;12:893-904.
13. Szymocha R, Akaoka H, Dutuit M, et al. Human T-cell lymphotropic virus type 1-infected T lymphocytes impair catabolism and uptake of glutamate by astrocytes via Tax-1 and tumor necrosis factor alpha. *J Virol.* 2000;74:6433-41.
14. Andersson T, Schwarcz R, Love A, et al. Measles virus-induced hippocampal neurodegeneration in the mouse: a novel. *Neurosci Lett.* 1993;154:109-12.
15. Wang GF, Li W, Li K. Acute encephalopathy and encephalitis caused by influenza virus infection. *Curr Opin Neurol.* 2010;23:305-11.
16. Kudo T, Fujii T, Ikegami S, et al. Mice lacking $\alpha 1,3$ -fucosyltransferase IX demonstrate disappearance of Lewis x structure in brain and increased anxiety-like behaviors. *Glycobiology.* 2007;17:1-9.
17. Taguchi F, Yamada A, Fujiwara K. Resistance to highly virulent mouse hepatitis virus acquired by mice after lowvirulence infection: enhanced antiviral activity of macrophages. *Infect Immun.* 1980;29:42-9.
18. Li YM, Baviello G, Vlassara H, et al. Glycation products in aged thioglycollate medium enhance the elicitation of peritoneal macrophages. *J Immunol Methods.* 1997;201:183-8.
19. Cook AD, Braine EL, Hamilton JA. The phenotype of inflammatory macrophages is stimulus dependent: implications for the nature of the inflammatory response. *J Immunol.* 2003;17:4816-23.
20. Misharin AV, Saber R, Perlman H. Eosinophil contamination of thioglycollate-elicited peritoneal macrophage cultures skews the functional readouts of in vitro assays. *J Leukoc Biol.* 2012;92:325-31.
21. Bogoevska V, Horst A, Klampe B, et al. CEACAM1, an adhesion molecule of human granulocytes, is fucosylated by fucosyltransferase IX and interacts with DC-SIGN of dendritic cells via Lewis x residues. *Glycobiology.* 2006;16:197-209.
22. Nishihara S, Iwasaki H, Nakajima K, et al. 3-Fucosyltransferase IX (Fut9) determines Lewis X expression in brain. *Glycobiology.* 2003;13:445-55.
23. Matsumura R, Hirakawa J, Sato K, et al. Novel antibodies reactive with sialyl Lewis X in both humans and mice define its critical role in leukocyte trafficking and contact hypersensitivity responses. *J Biol Chem.* 2015;290:15313-26.
24. Gallily R, Warwick A, Bang FB. Effect of cortisone on genetic resistance to mouse hepatitis virus in vivo and in vitro. *Proc Natl Acad Sci U S A.* 1964;51:1158-64.
25. Ghosn EE, Cassado AA, Govoni GR, et al. Two physically, functionally, and developmentally distinct peritoneal macrophage subsets. *Proc Natl Acad Sci U S A.* 2010;107:2568-73.
26. Schleicher U, Hesse A, Bogdan C. Minute numbers of contaminant CD8 + T cells or CD11b + CD11c + NK cells are the source of IFN- γ in IL-12/IL-18-stimulated mouse macrophage populations. *Blood.* 2005;105:1319-28.
27. Vodovotz Y, Bogdan C, Paik J, et al. Mechanisms of suppression of macrophage nitric oxide release by transforming growth factor β . *J Exp Med.* 1993;178:605-13.
28. Schindler H, Lutz MB, Rollingshoff M, et al. The production of IFN- γ by IL-12/IL-18-activated macrophages requires STAT4 signaling and is inhibited by IL-4. *J Immunol.* 2001;166:3075-82.
29. Nakagaki K, Nakagaki K, Taguchi F. Receptor-independent spread of a highly neurotropic murine coronavirus JHMV strain from initially infected microglial cells in mixed neural cultures. *J Virol.* 2005;79:6102-10.
30. Ribechini E, Greifengberg V, Sandwick S, et al. Subsets expansion and activation of myeloid-derived suppressor cells. *Med Microbiol Immunol.* 2010;199:273-81.
31. Dijkman R, Jebbink MF, Deijs M, et al. Replication-dependent downregulation of cellular angiotensin-converting enzyme 2 protein expression by human coronavirus NL63. *J Gen Virol.* 2012;93:1924-9.
32. Boscher C, Dennis JW, Nabi IR. Glycosylation, galectins and cellular signaling. *Curr Opin Cell Biol.* 2011;23:383-92.
33. Rabinovich GA, van Kooyk Y, Cobb BA. Glycobiology of immune responses. *Ann N Y Acad Sci.* 2012;1253:1-15.
34. van Kooyk Y, Rabinovich GA. Protein-glycan interactions in the control of innate and adaptive immune responses. *Nat Immunol.* 2008;9:593-601.
35. Gringhuis SI, den Dunnen J, Litjens M, et al. Carbohydrate-specific signaling through the DC-SIGN signalosome tailors immunity to Mycobacterium tuberculosis, HIV and Helicobacter pylori. *Nat Immunol.* 2009;10:1081-8.
36. Samsen A, Bogoevska V, Klampe B, et al. DC-SIGN and SRCL bind glycans of carcinoembryonic antigen (CEA) and CEA-related cell adhesion molecule 1 (CEACAM1): recombinant human glycan-binding receptors as analytical tools. *Eur J Cell Biol.* 2010;89:87-94.
37. Johnson JL, Jones MB, Ryan SO, et al. The regulatory power of glycans and their binding partners in immunity. *Trends Immunol.* 2013;34:290-8.
38. Gracia-Vallejo JJ, Ilarregui JM, Kalay H, et al. CNS myelin induces regulatory functions of DC-SIGN-expressing, antigen-presenting cells via cognate interaction with MOG. *J Exp Med.* 2014;211:1465-83.
39. Kawachi Y, Takagi H, Hanafusa K, et al. SIGNR1-mediated phagocytosis, but not SIGNR1-mediated endocytosis or cell adhesion, suppresses LPS-induced secretion of IL-6 from murine macrophages. *Cytokine.* 2015;71:45-53.
40. Kashiwazaki H, Taguchi F, Ikehara Y, et al. Characterization of splenic cells during the early phase of infection with neuropathogenic mouse hepatitis virus. *Jpn J Infect Dis.* 2011;64:256-9.
41. Nomura R, Kashiwazaki H, Kakizaki M, et al. Receptor-independent infection by mutant viruses newly isolated from the neuropathogenic mouse hepatitis virus srr7 detected through a combination of spinoculation and ultraviolet radiation. *Jpn J Infect Dis.* 2011;64:499-505.
42. Lee SJ, Hori Y, Groves JT, et al. Correlation of a dynamic model for immunological synapse formation with effector function: two pathways to synapse formation. *Trends Immunol.* 2002;23:492-9.
43. Pittet MJ, Nahrendorf M, Swirski FK. The journey from stem cell to macrophage. *Ann NY Acad Sci.* 2014;1319:1-18.